Low-loss D-shape Silicon Nitride Waveguides Using a Dielectric Lift-off Fabrication Process

Qiancheng Zhao[1], Jiawei Wang[1], Nitesh Chauhan[1], Debapam Bose[1], Naijun Jin[2], Renan Moreira[1], Ryan Behunin[4], Peter Rakich[2] and Daniel Blumenthal[1*]

[1]Department of Electrical and Computer Engineering, University of California, Santa Barbara, CA, USA, 93106
[2]Department of Applied Physics, Yale University, New Haven, CT, USA, 06511
[4]Department of Applied Physics and Material Sciences, Northern Arizona University, Flagstaff, AZ, USA, 86011
**danb@ucsb.edu*

Abstract: D-shape Si_3N_4 waveguides are fabricated by dielectric lift-off process. We measure ultra-low loss for a 90nm-thick core of 2.42 dB/m at 1550 nm and a loaded Q-factor of 1.12×10^6 for a 0.8 mm radius resonator. © 2020 The Author(s)

OCIS codes: (230.7390) waveguides, planar; (250.5300) photonic integrated circuits.

1. Introduction

Low-loss waveguides enable a broad range of photonic integrated circuits (PICs) such as integrated optical gyroscopes [1], atomic clocks [2], narrow-linewidth SBS lasers [3], and optical frequency combs [4]. The performance of these applications requires waveguides with sub-dB/cm propagation loss. Numerous efforts have been devoted to identifying and addressing the limiting factors of waveguide losses [5], among which waveguide sidewall roughness is a dominant factor. Elimination of the sidewall roughness is a key approach to lowering losses.

Waveguide sidewall roughness, often caused by dry etching, can be mitigated by several techniques including Damascene reflow [6], photoresist thermal reflow [7], laser annealing [8] and dielectric lift-off. The dielectric lift-off process is usually implemented by depositing a waveguiding structure that has smoother sidewalls. This method is CMOS-compatible and is scalable to large areas, and it has been used in reducing chalcogenide [9] and titanium dioxide [10] waveguide propagation losses. Here we demonstrate a low-loss D-shape high-aspect-ratio silicon nitride (Si_3N_4) waveguide using a silicon dioxide (SiO_2) hardmask created by the dielectric lift-off process. The waveguide propagation loss is 2.42 dB/m at 1550 nm. A loaded Q-factor of 1.12×10^6 is measured for a 0.8 mm radius resonator. This is the first demonstration of the D-shape high-aspect-ratio Si_3N_4 waveguides. The method of patterning SiO_2 hardmask by the dielectric lift-off process can be applied to other waveguide core materials.

2. Device Fabrication

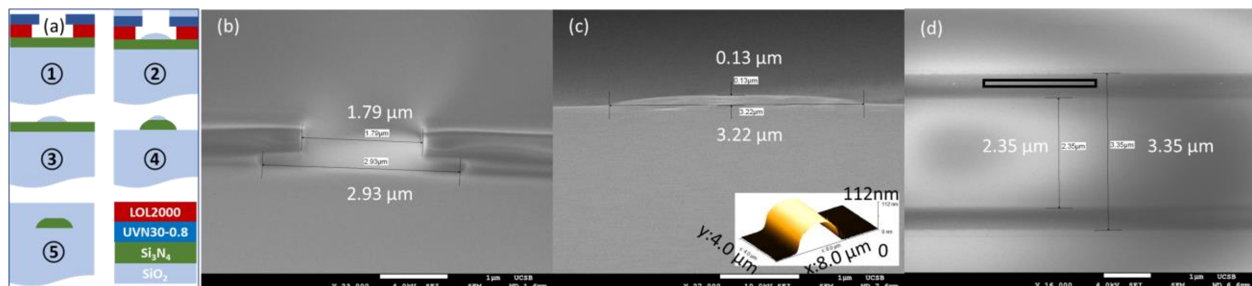

Fig. 1 (a) Dielectric lift-off process flow. Cross section view of the bilayer-resist undercut (b) and a 3μm-wide etched D-shape waveguide (c). The inset in (c) shows the AFM image of an 8μm-wdie D-shape SiO_2 hardmask. (d) is the top view of the etched 3μm-wide D-shape waveguide

The fabrication process, illustrated in Fig. 1(a), starts with depositing a 90 nm stoichiometric LPCVD Si_3N_4 film on a thermal oxide (15 μm) silicon (Si) wafer. A ~250 nm LOL2000 lift-off layer and ~550 nm UVN30-0.8 photoresist layer are spin-coated sequentially on the wafer and get exposed by an ASML DUV Stepper. The undercut depth in the LOL2000 layer is controlled by the photoresist developing time, and ~570 nm undercut (Fig. 1(b)) is measured in our experiment to avoid wings after lift-off. A layer of 112 nm SiO_2 is deposited on the photoresist-patterned wafer by RF sputtering Si with oxygen flow. The SiO_2 layer is lifted off by immersing the wafer in n-methyl-2-pyrrolidone (NMP) solvent with ultrasonic heat bath. Special attention has been paid to thoroughly wash the wafer to minimize particle contaminations. The D-shape of the hardmask is transferred into the waveguide core layer by using fluorine-based dry etching. Since the etching ratio of the SiO_2 to Si_3N_4 is close to 1, a one-to-one copy of the D-shape from the hardmask to the waveguide core can be obtained, as shown in Fig. 1(c). A 6 μm SiO_2 upper cladding layer is deposited afterwards, and the wafer is annealed above 1050°C to reduce material loss.

3. Waveguide characterization

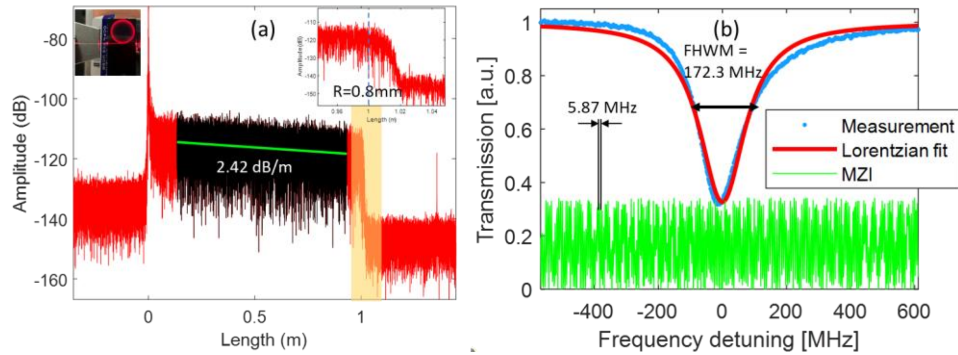

Fig. 2 (a) OBR data from a 1-meter long spiral delay. The top left inset shows the waveguiding using a red laser. The top right inset shows the loss caused by small bending radius. The dashed line approximates where 0.8 mm radius is along the spiral line. (b) Transmission spectrum of an 0.8 mm radius all-pass ring resonator.

The bottom width of the D-shape waveguide is ~0.3 µm wider than the design due to the extruding of the SiO_2 hardmask into the photoresist undercut layer, as shown in Fig. 1(c) and (d). Consequently, the D-shape waveguide has a flatter sidewall surface slope than rectangular waveguide. The sidewall surface is measured to have a RMS roughness S_q = 607.2 pm and an average roughness S_a = 467.0 pm by AFM in the black boxed region in Fig. 1(d). There are still SiO_2 hardmasks left on top of the Si_3N_4 layer after dry etching (shown in Fig. 1(d)), and they will be buried into the SiO_2 upper cladding layer, leaving negligible discontinuities.

To quantify the propagation loss, optical backscatter reflectometry (OBR) is employed to scan a wide range of spectrum (1525-1610 nm) into a 1 meter-long and 3 µm-wide spiral waveguide, enabling 0.1 µm-level spatial resolution. Fig.2 (a) shows the reflection amplitude measured from the spiral delay, and the propagation loss is curve fitted to be 2.42 dB/m, which is lower than the previous reported value for 90 nm Si_3N_4 waveguides of 4.22 dB/m [11] and 4.65 dB/m [12], The spiral radius shrinks from 4.05 mm to 121.8 µm from outside to inner. As a result, the propagation loss increases when the light travels towards the end of the spiral due to small radii, as shown in the top right inset in Fig.2 (a). The dashed line approximates where R = 0.8 mm is at the spiral delay, beyond which the reflected signal starts to drop sharply due to bending loss. The propagation loss is also verified using the Q-factor (Fig.2 (b)) of a bus-coupled ring resonator that has a radius of 0.8 mm. The loaded Q was measured by using a calibrated unbalanced MZI with FSR of 5.87 MHz. The FWHM of the resonance is 172.31 MHz with a loaded Q of 1.12×10^6 at 1550 nm. The gap of the resonator is ~1.7 µm and the coupling coefficient is estimated to be 2.45% from measurements. The propagation loss of the resonator is derived to be 2.98 dB/m. The slightly higher loss from Q measurement than from the OBR results can be attributed to that the bending loss starts to become noticeable. If bending loss could be neglected and assuming a critical coupling, a Q of 5.6×10^6 should be expected with the measured loss from OBR. Considering the ring radius is close to critical bend radii for 90 nm Si_3N_4 strip waveguides [13], the propagation loss of the D-shape waveguide is reasonably low, enabling the possibility for compact integration. In summary, we demonstrate the D-shape high-aspect-ratio waveguides fabricated by dielectric lift-off process which shows lower propagation loss than records.

Acknowledgment and funding information: This work was supported by DARPA MTO APhI contract number FA9453-19-C-0030. The views, opinions and/or findings expressed are those of the author(s) and should not be interpreted as representing the official views or policies of the Department of Defense or the U.S. Government.

[1] Sarat Gundavarapu et al., J. Lightwave Technol., vol. 36, no. 4, pp. 1185–1191, Feb. 2018.
[2] Andrew D. Ludlow et al., Rev. Mod. Phys., vol. 87, no. 2, pp. 637–701, Jun. 2015.
[3] Sarat Gundavarapu et al., Nature Photon, vol. 13, no. 1, pp. 60–67, Jan. 2019.
[4] Junqiu Liu et al., Optica, vol. 5, no. 10, pp. 1347–1353, Oct. 2018.
[5] Martin H. P. Pfeiffer et al., Optica, vol. 5, no. 7, pp. 884–892, Jul. 2018.
[6] Martin H. P. Pfeiffer et al., IEEE Journal of Selected Topics in Quantum Electronics, vol. 24, no. 4, pp. 1–11, Jul. 2018.
[7] Gyorgy A. Porkolab et al., Opt. Express, vol. 22, no. 7, pp. 7733–7743, Apr. 2014.
[8] Qiangfei Xia et al., Nanotechnology, vol. 20, no. 34, p. 345302, Aug. 2009.
[9] Juejun Hu et al., Opt. Express, OE, vol. 15, no. 19, pp. 11798–11807, Sep. 2007.
[10] Christopher C. Evans et al, Opt. Express, vol. 23, no. 9, pp. 11160–11169, May 2015.
[11] Jared F. Bauters et al., Opt. Express, vol. 19, no. 4, pp. 3163–3174, Feb. 2011.
[12] Chao Xiang et al., IEEE Journal of Selected Topics in Quantum Electronics, vol. 24, no. 4, pp. 1–9, Jul. 2018.
[13] Daniel J. Blumenthal et al., Proceedings of the IEEE, vol. 106, no. 12, pp. 2209–2231, Dec. 2018.